EINDHOVEN UNIVERSITY OF TECHNOLOGY

Silicon etch rate enhancement by traces of metal

Citation for published version (APA):
Sebel, P. G. M., Hermans, L. J. F., & Beijerinck, H. C. W. (1999). Silicon etch rate enhancement by traces of metal. *Journal of Vacuum Science and Technology A*, *17*(3), 755-762. https://doi.org/10.1116/1.581645

DOI:
10.1116/1.581645

Document status and date:
Published: 01/01/1999

Document Version:
Publisher's PDF, also known as Version of Record (includes final page, issue and volume numbers)

Please check the document version of this publication:

• A submitted manuscript is the version of the article upon submission and before peer-review. There can be important differences between the submitted version and the official published version of record. People interested in the research are advised to contact the author for the final version of the publication, or visit the DOI to the publisher's website.
• The final author version and the galley proof are versions of the publication after peer review.
• The final published version features the final layout of the paper including the volume, issue and page numbers.

Link to publication

General rights
Copyright and moral rights for the publications made accessible in the public portal are retained by the authors and/or other copyright owners and it is a condition of accessing publications that users recognise and abide by the legal requirements associated with these rights.

• Users may download and print one copy of any publication from the public portal for the purpose of private study or research.
• You may not further distribute the material or use it for any profit-making activity or commercial gain
• You may freely distribute the URL identifying the publication in the public portal.

If the publication is distributed under the terms of Article 25fa of the Dutch Copyright Act, indicated by the "Taverne" license above, please follow below link for the End User Agreement:

www.tue.nl/taverne

Take down policy
If you believe that this document breaches copyright please contact us at:

openaccess@tue.nl

providing details and we will investigate your claim.

Download date: 16. Nov. 2023

Silicon etch rate enhancement by traces of metal

P. G. M. Sebel, L. J. F. Hermans, and H. C. W. Beijerinck[a)]
Physics Department, Eindhoven University of Technology, 5600 MB Eindhoven, The Netherlands

(Received 9 July 1998; accepted 2 January 1999)

We report the effect of nickel and tungsten contamination on the etch behavior of silicon. This is studied in a molecular beam setup, where silicon is etched by XeF_2 and Ar^+ ions. The etch process is directly monitored by the SiF_4 reaction products which leave the surface. The effect of contamination appears very pronounced after the ion beam is switched off: it leads to a temporary enhancement of the spontaneous etch rate on a time scale of 500 s. With traces of contamination on the order of 0.01 ML, the etch rate may be enhanced by a factor of 2 for W and somewhat less for Ni. It is concluded that the contamination moves into the silicon by diffusion to vacancies created by the Ar^+ ions. For 1 keV Ar^+ ions the contamination moves to a depth of 25 Å, comparable to the penetration depth of the ions. After etching a 170 Å thick layer, the catalytic effect of contamination is reduced to less than 5%. A simple model, which describes the measured effect of contamination very well, indicates that only 3% of the contamination is removed when a monolayer of silicon is etched away. Besides this catalytic effect there are indications that contamination can also lower the etch rate under certain conditions, because of the formation of silicides. From the measurements no conclusions could be drawn about the underlying mechanism of etch rate enhancement. © *1999 American Vacuum Society.* [S0734-2101(99)01103-3]

I. INTRODUCTION

During the production of an integrated circuit, a wafer can suffer several types of contamination which may influence the next step in the process and the final reliability of the device. As dimensions of features are still decreasing, damage to the wafer becomes more critical. The main form of contamination consists of traces of metal, sputtered from walls or electrodes, which are deposited on the surface of a wafer. Depending on the type of reactor and materials used for electrodes, traces of Ca, Fe, Zn, Cr, Mn, Ni, Cu, and K in the range from 0.01 to 0.4 ML may be found on the wafer after etching. Even after extensive cleaning some of these contaminants remain on the surface.[1] Another source of contamination consists of solutions used for, e.g., resist development which may leave traces of Na and K on the surface.[2,3] The increasing concern about contaminants is illustrated by the development of sensitive equipment to detect even smaller traces of contamination.[4]

As we focus on the effect of contamination on the etch behavior, the intentional doping of silicon with, e.g., B or P may also be regarded as contamination of the wafer. Contamination can have different effects on the etch behavior. Some contaminants (e.g., B[2]) reduce the etch rate, but most contaminants (K, Na;[2,3] Cu;[5,6] and P[7]) increase the etch rate. The effect of metal contamination has so far only been studied for Cu on silicon. Some monolayers of Cu may increase the etch rate of silicon by F_2 by a factor of 100 at temperatures above 60 °C. At room temperature no significant effect was reported.[5,6] The contamination of Cu can also result in anisotropic etching.[6] The effect of tungsten contamination has been described briefly in an appendix of an article by Vugts *et al.*[8] and the authors initially attributed the effect to damage-enhanced etching.[9]

In this study we report on the effect of nickel contamination on the etch behavior of silicon by XeF_2 and Ar^+ ions at room temperature. The effect of contamination is found to be very pronounced when the Ar^+ ions are switched off. Under clean conditions, the etch rate drops to the spontaneous etch level within several seconds after the Ar^+ ions have been switched off. In the presence of contamination, the etch rate also drops initially, but then increases temporarily and reaches the steady state situation of spontaneous etching again on a time scale of 500 s.

In Sec. II the experimental setup and the sources of contamination are described. In Sec. III, the effect of nickel contamination is studied as function of XeF_2 flux, ion flux and ion energy. As a function of these parameters, the effect of the contamination changes. This observed behavior is explained in Sec. IV by a diffusion process of the contaminants to vacancies produced by the Ar^+ ions in the silicon. This mechanism is simulated with a simple model which describes the observed behavior very well. Furthermore, previously measured contamination effects of tungsten[9] are compared with those caused by nickel. This leads to a consistent picture of the influence of metal contamination. In Sec. VI the conclusions are summarized.

II. EXPERIMENTAL SETUP

A. Apparatus

The multiple-beam setup is described in detail by Vugts *et al.*[10] We limit ourselves to a brief description of the key features used in this study.

The silicon sample is placed at the intersection of the XeF_2 beam and the Ar^+ beam in an UHV chamber (10^{-8}

[a)]Electronic mail: H.C.W.Beijerinck@phys.tue.nl

 ©1999 American Vacuum Society

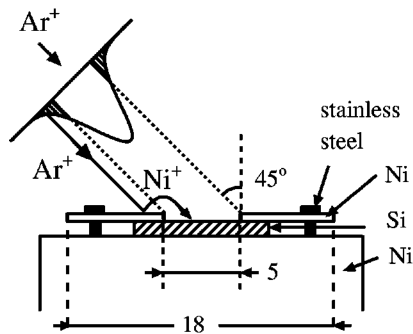

FIG. 1. Sample holder. The various sizes of the components are indicated in mm. As the Ar^+ ion beam partly hits the nickel retainer plate, Ni^+ can be sputtered and deposited on the Si sample (hatched) by a bias voltage of −100 V.

mbar) on a temperature controlled sample holder (100–1000 K). In this study, all measurements are performed at room temperature. The Si(100) samples (n type, phosphorus, 2–3 Ω cm) are cleaned with HF to remove native oxide before being mounted. Several samples are used during the experiments. The XeF_2 beam and Ar^+ beam are incident under 52° and 45°, respectively, with respect to the surface normal. The sample is attached to the electrically insulated sample holder by a nickel retainer plate, with an opening of 5 mm in diameter (Fig. 1).

The XeF_2 gas is supplied by a multi-capillary effusive gas source. During the experiments a XeF_2 flux $\Phi_s(XeF_2)$ of 2 and 3 ML s^{-1} is used. For silicon 1 ML corresponds to 6.86×10^{18} m^{-2}. For the Ar^+ beam, the ion energy is 1 keV, and its intensity is given in terms of the total ion current in μA hitting the Si sample and Ni retainer plate (Fig. 1 and Sec. III). The ion current is not corrected for the influence of the emission of secondary electrons.

The etch reaction is monitored by a quadrupole mass spectrometer (QMS) in a separate UHV chamber ($<10^{-8}$ mbar) positioned along the surface normal of the sample. The central detection area (CDE) seen by the QMS is 3 mm in diameter. With the mass spectrometer, the nonreacted XeF_2 flux $\Phi(XeF_2)$ (XeF^+ signal) and the reaction product SiF_4 (SiF_3^+ signal) are measured. From the XeF_2 flux $\Phi_s(XeF_2)$ leaving the inert Ni and the nonreacted XeF_2 flux $\Phi(XeF_2)$ leaving the Si surface, the reaction probability ϵ of the XeF_2 is calculated

$$\epsilon=\frac{\Phi_s(XeF_2)-\Phi(XeF_2)}{\Phi_s(XeF_2)}. \tag{1}$$

The SiF_4 signal yields the production coefficient δ, defined by

$$\delta=\frac{4\Phi(SiF_4)}{2\Phi_s(XeF_2)}. \tag{2}$$

As SiF_4 is the only reaction product at room temperature, it follows from the F-atom balance that $\epsilon=\delta$ in a steady-state situation, which is used as a calibration of the production coefficient δ. The silicon etch rate R (ML/s) at any moment is now easily calculated by

$$R=\Phi(SiF_4)=\frac{\delta}{2}\Phi_s(XeF_2). \tag{3}$$

For Si(100) the etching of 1 ML corresponds to a depth of 1.38 Å. Equation (3) only holds for spontaneous etching at room temperature. For ion-assisted etching SiF_2 is also produced and this has to be taken into account in the F-atom mass balance.[8]

B. Sources of contamination

1. Nickel

The nickel retainer plate used to clamp the silicon sample (Fig. 1) was found to act as a source of Ni contaminants, since Ni is sputtered from this cover under ion bombardment. The sputter yield is 1.7 atoms/ion for Ni when bombarding with 1 keV Ar^+ ions at normal incidence.[11] Ni^+ ions will also be sputtered[12,13] and by applying a negative bias (−100 V in our experiments), these ions can be deflected towards the silicon. The nickel contamination was confirmed by low-energy ion scattering measurements as a diagnostic tool (see Sec. III). The measurements were performed in a setup similar to the energy resolved ion scattering spectrometry (ERISS) setup with 5 keV Ne^+ ions.[14] With this method only the top layer of the sample is analyzed and a low ion current is being used to prevent damage to the sample. Deeper layers have been analyzed after the silicon has been sputtered by Ne^+ ions with a higher current.

2. Tungsten

The source of tungsten contamination (reported previously[8]) is an ionization gauge. The tungsten filament of the gauge reacts with residual XeF_2 which results in the formation of WF_6. This process is enhanced by electron and ion impact.[15] Thus a background of WF_6 is formed in the vessel and WF_6 can be deposited on the Si, although the gauge is completely out of sight of the sample. No WF_x^+ signal in the mass spectrometer was reported,[8,9] but the signal is probably below detection limit. The contamination by WF_6 can be eliminated by a liquid N_2 vessel which acts as a cryopump for both XeF_2 and WF_6. In contrast to the Ni contamination, which is produced only if the ion beam is on, this W is ever present when the ionization gauge is switched on. During the measurements presented here, the ionization gauge was always switched off and the liquid N_2 vessel was filled.

III. EXPERIMENTAL RESULTS

A. Etch behavior

Figure 2 shows the response of the production coefficient δ when the Ar^+ ions are switched off. In the upper graph no contamination is present and, within a few seconds, the production coefficient δ drops to the production coefficient measured before the ion bombardment. However, in the presence of nickel contamination (see Sec. III C), the SiF_4 production is temporarily enhanced (lower graph of Fig. 2). On a time scale of 500 s the spontaneous value is recovered. For the

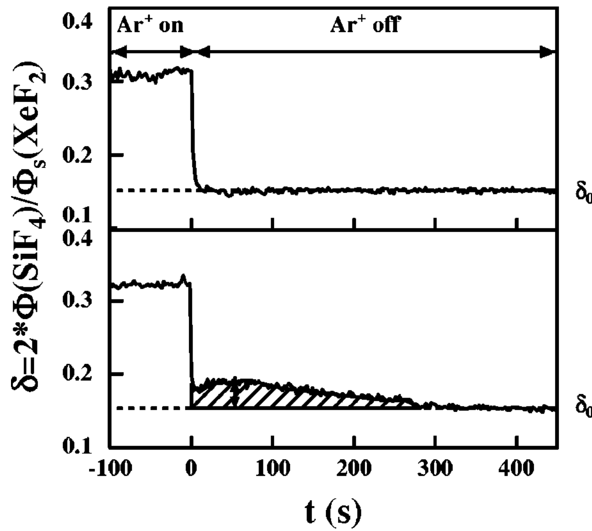

FIG. 2. Effect of contamination on the production coefficient δ for SiF_4. On $t=0$ the Ar^+ ions are switched off. In case of a clean surface (upper plot), the etch rate drops immediately to the spontaneous value δ_0. In the presence of contamination we observe a temporary increase (hatched area) until the steady-state value δ_0 is reached after 500 s. The maximum increase at $t=60$ s varies, depending on the specific conditions. The maximum enhancement may even become equal to the ion-assisted etch rate.

measurements described here, the production coefficient δ_0 of SiF_4 for spontaneous etching in a steady-state situation was measured to be

$$\delta_0 = 0.15 \pm 0.03. \tag{4}$$

In Fig. 3 the influence of the XeF_2 flux is shown for 2 and 3 ML/s. In these measurements the sample was bombarded with ions for 60 s. To compare the different fluxes, the time axis t is replaced by the total dose $\mathcal{D}$ of XeF_2 that reached the sample after the ions have been switched off

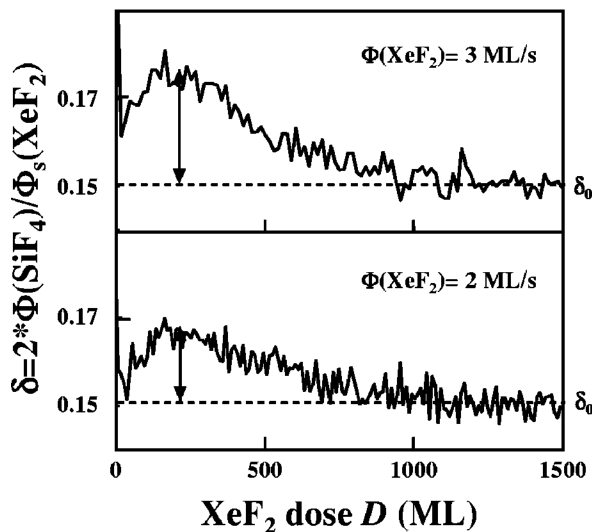

FIG. 3. Influence of the XeF_2 flux on the enhancement of the production coefficient. The horizontal scale is the total dose of XeF_2 after the ions have been switched off. Measurements are shown for XeF_2 fluxes of 2 and 3 ML/s.

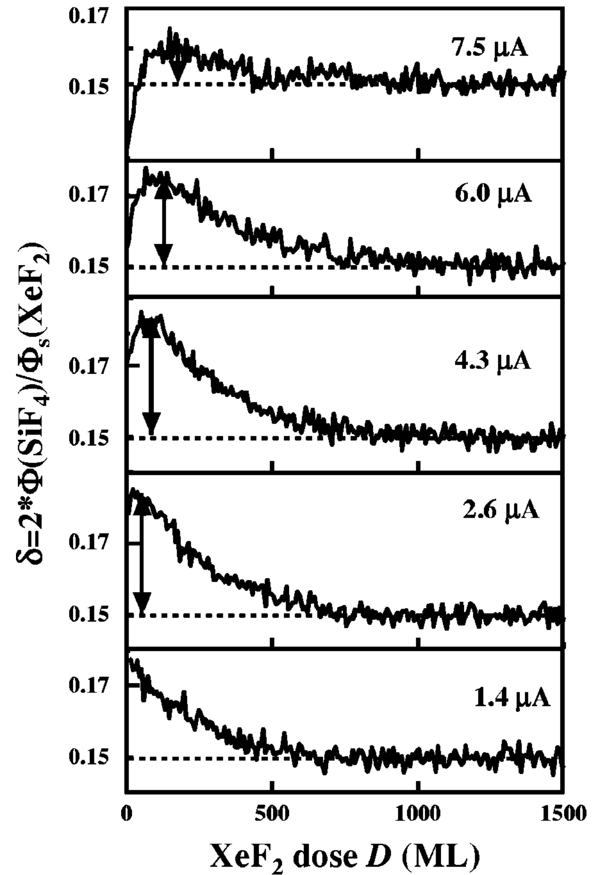

FIG. 4. Influence of the ion current. Shown is the response after the ion beam is switched off, for various ion currents with bombardment time $T_{ion}=180$ s.

$$\mathcal{D} = \Phi_s(XeF_2) \times t. \tag{5}$$

From the measurements it is seen that the temporary enhancement appears for both fluxes at the same dose of XeF_2. The maximum enhancement during the experiments differs with time and sample. From the measurements of the beam shape, it is concluded that this can be explained by differences in the shape of the ion beam caused by differences in the argon gas feed in the ion source.

We conclude that the source of the enhancement is located in a layer that needs to be removed by etching before the enhancement disappears. It is easily calculated that the maximum enhancement is reached after etching 18 ± 5 ML (25 Å) and that the effect of contamination is reduced to less than 5% after 120 ± 15 ML (170 Å) has been etched away.

In Fig. 4 the influence of the ion current is shown. The sample was bombarded with ions for 180 s. It thus follows that the maximum enhancement is reached after a number of Si layers has been removed, ranging from 30 ML for the highest currents to almost zero at 1.4 μA. The maximum enhancement, however, drops for higher ion currents. For the highest ion current, δ even drops below the spontaneous value δ_0 immediately after the ions have been switched off.

The influence of the ion bombardment time T_{ion} on the etch rate enhancement is shown in Fig. 5. These measurements were done for an ion current of 6 μA. The maximum

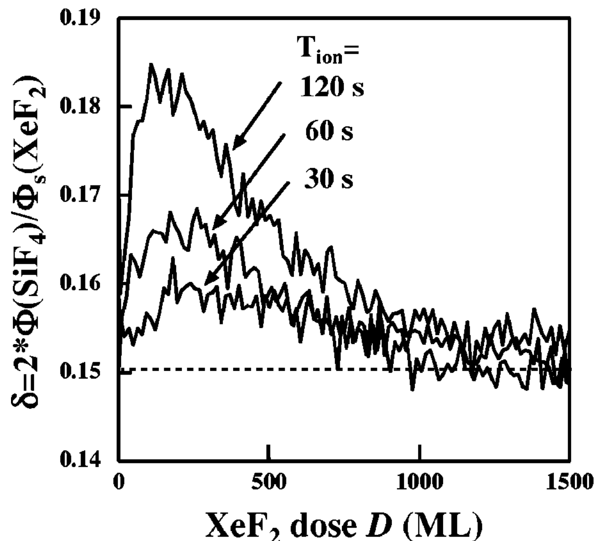

FIG. 5. Enhancement for various values of the ion bombardment time T_{ion}. Shown is the response after bombardment times of 30, 60, and 120 s at an ion current of 6 μA.

enhancement increases with increasing bombardment time, but appears after about the same dose of XeF_2.

The influence of ion energy is shown in Fig. 6. The measurements were done with an ion current of 6 μA during 60 s. It is clearly shown that the point of maximum enhancement moves deeper into the silicon for higher energy. Also, directly after switching off the ions, the etch rate drops below the spontaneous rate for the 2.5 keV ions. The same effect was measured for the highest ion current as shown in Fig. 4.

B. Measurements of the ion beam shape

In order to confirm the sputtering of nickel from the retainer plate, the shape of the ion beam is analyzed in a separate experiment. This is done by mounting a wire (double wound 0.5 mm Ni wire) vertically on the sample holder instead of a silicon sample. The wire is electrically insulated from the sample holder and placed 2 mm above it. The current of the ion beam hitting the wire (in the order of nA) is measured with an electrometer. In Fig. 7 the shape of the ion beam is shown. The beam has a Gaussian central peak with a width of 5 mm and a very broad background. The asymmetric dip in ion current around $x=-8$ mm is explained by the influence of secondary electrons. These electrons are emitted in forward direction with respect to the ion beam, incident at 45°, from the sample holder behind the scanning wire. These electrons thus have a maximum influence on the total measured current when the ion beam is on the left of the scanning wire and the electrons are ''reflected'' to the wire. From this beam profile, we see that about 50% of the ions hits the nickel retainer plate, since the ion beam is much wider than the exposed silicon sample with a diameter of 5 mm. In later experiments, the broad wings of the ion beam profile could be reduced by using a higher argon pressure in the ion source and improving the focus and width of the ion beam.

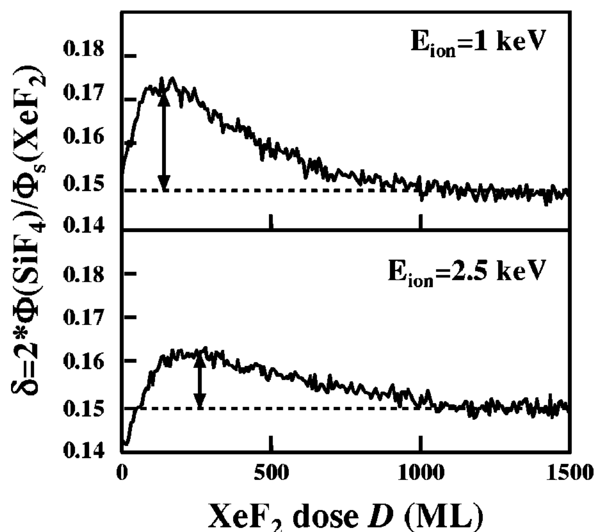

FIG. 6. Influence of the ion energy on the enhancement. The average response of three measurements is shown for 1 and 2.5 keV Ar^+ ions after the Si is bombarded with a 6 μA ion current for 60 s.

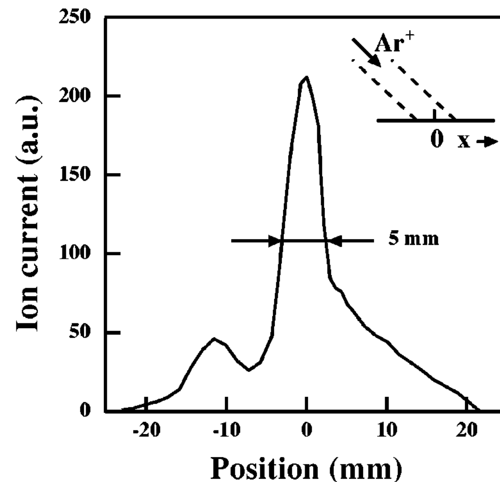

FIG. 7. Ion beam profile as measured with a wire scanner of width 1 mm. The graph shows the profile as used for the measurements in this article.

C. Surface analysis

An etched Si sample used for the measurements described in the previous section was taken out for surface analysis. This sample was etched for 1000 s at a XeF_2 flow of 3 ML/s and a 1 keV ion beam of 6.0 μA, after the surface was cleaned from previous runs by spontaneous etching. The XeF_2 flow and ion current were stopped simultaneously. Low-energy ion scattering spectroscopy (LEIS) measurements showed no contamination on the surface. A repeated measurement after sputtering a layer with a depth of an estimated 30 Å showed a nickel concentration of approximately 0.01 ML. This nickel contamination together with the beam shape confirms the earlier conclusion that sputtered nickel from the retainer plate causes the observed etch behavior displayed in Figs. 3–6.

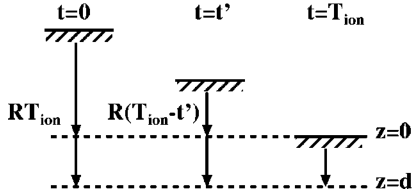

FIG. 8. Schematic view of the surface position during ion-enhanced etching, as used for the calculation of the steady-state vacancy distribution during ion-assisted etching from $t=0$ to $t=T_{\mathrm{ion}}$. The depth d is defined with respect to the surface position at $t=T_{\mathrm{ion}}$ when the etching is stopped.

IV. DISCUSSION

A. Mechanism of enhancement by contamination

In the previous section, the measurements show that the appearance of the enhancement clearly depends on the ion bombardment. The effect of ions on contaminants deposited on a surface of silicon has been described by Hart *et al.*[16] After deposition of 0.13 ML Cu on Si, they found that copper, when bombarded with 20 keV Ne^+ ions, moves into the silicon as deep as 600 Å instead of being sputtered. When successively bombarding this silicon with 800 eV Ar^+ ions, they found that copper moves back towards to surface to a depth of less than 125 Å. From these results it was concluded that the copper moves into the silicon by the mechanism of enhanced diffusion by defect production, these defects being created in the silicon by the energetic ions. The copper atoms thus migrate to depths comparable to the penetration depth of the incident ions.

This mechanism of enhanced diffusion presumably also causes the nickel contamination to move into the silicon. In order to further corroborate this conjecture, we developed a model. To simulate the vacancy distribution for 1 keV Ar^+ ions as a function of the depth d we use the ''TRIM'' program developed by IBM.[17] The ion angle is set at 45° with respect to the surface normal, in agreement with the experimental setup. The vacancy distribution $v(d)$ (Å^{-1}) as calculated with TRIM is transformed to an average distribution $\langle v(d)\rangle$ to include the movement of the surface due to the etching with a rate $R=0.5\ \delta\ \Phi_s(\mathrm{XeF_2})$. This procedure is schematically shown in Fig. 8. The ion bombardment starts at $t=0$ and ends at $t=T_{\mathrm{ion}}$. Since a depth $z=d$ at $t=T_{\mathrm{ion}}$ corresponds to a depth $d+RT_{\mathrm{ion}}$ at $t=0$, the average vacancy distribution is calculated by integration over this range of depths, that contributes to the creation of vacancies at the final depth $z=d$:

$$\langle v(d)\rangle_{T_{\mathrm{ion}}}=\frac{1}{T_{\mathrm{ion}}}\int_0^{T_{\mathrm{ion}}} v[d+(T_{\mathrm{ion}}-t')R]dt'. \quad (6)$$

A steady-state distribution is reached when $RT_{\mathrm{ion}}>d_{\max}$, with $d_{\max}$ the maximum penetration depth of the ions. In Fig. 9 the calculated vacancy distribution $v(d)$ (solid line) is shown as well as the steady-state distribution $\langle v(d)\rangle$ (dotted line) for 1 keV Ar^+ ions on silicon. Since a steady-state distribution is reached in our experiments after about 30 s of ion-assisted etching, this distribution is used.

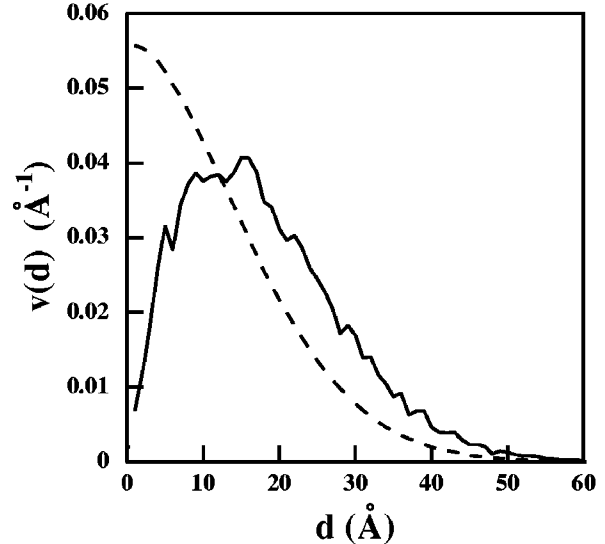

FIG. 9. Solid line: vacancy distribution $v(d)$ calculated with TRIM for 1 keV Ar^+ ions incident at 45°. The dashed line corresponds to the steady-state vacancy distribution when the movement of the surface is included.

From our etching results it was concluded that the maximum enhancement appears after etching a layer with thickness of about 18 ML. From Fig. 9 it can be seen that, at this depth, the concentration of vacancies has been reduced to 10% of its value at the surface. Thus the maximum enhancement corresponds very well to the depth range of the vacancies. It was also observed that the effect of contamination disappears only after etching of 120 ML. This is much deeper than the ion range. We conclude that a large fraction of the nickel is not etched but remains on the surface. Nickel thus has a catalytic effect on the etch rate of silicon. This explains that the position of the maximum enhancement corresponds to $d_{\max}$, since at this point all nickel in the sample has been accumulated on the surface. Figure 6 shows that increasing $d_{\max}$ of the ions by increasing the ion energy indeed causes the nickel to move deeper in the silicon.

The above description is correct only if the diffusion of the nickel atoms is fast enough to follow the movement of the surface and the vacancy distribution. Only under these conditions will the nickel move as deep as the ion penetration depth $d_{\max}$. As the diffusion is assumed to be governed by the vacancy mechanism, the diffusion coefficient should increase with the vacancy concentration[18] and thus with ion current or ion energy. Consequently, as a function of the ion current, the nickel should move deeper into the silicon. This can indeed be seen in Fig. 4, where the maximum enhancement and thus the nickel moves deeper in the silicon with increasing ion current.

B. Model

To obtain more insight in the process of etching in the presence of contamination, the measurements were simulated with a simple model. The nickel diffusion is assumed to be fast enough to follow the moving surface. The average vacancy distribution $\langle v(d)\rangle$ is thus used as the distribution

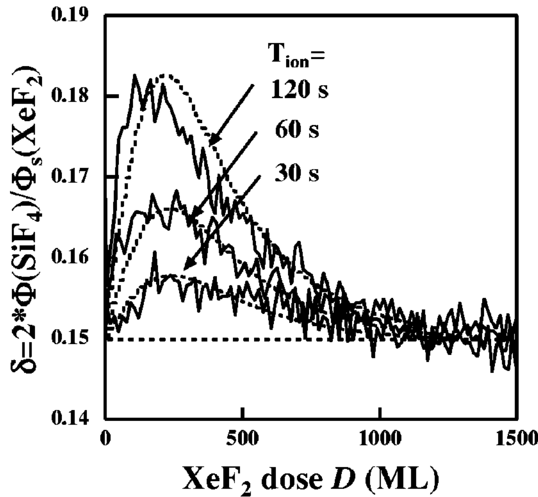

FIG. 10. Results of the simulation (dotted curves) of the temporary enhancement by nickel contamination for various bombardment times for the data of Fig. 5.

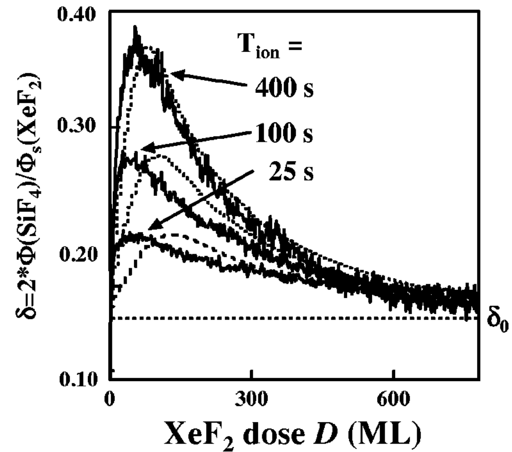

FIG. 11. Measurements (solid curves) and simulation (dotted curves) for the temporary enhancement due to tungsten contamination. The parameter α, determining the maximum enhancement, is manually adjusted to compensate for the saturation of the maximum enhancement as a function of T_{ion}.

function for the Ni contaminants. The total etch rate is given by the sum of the spontaneous etch rate [Eq. (3)] and the enhancement due to the nickel contamination. The enhancement is assumed to be linear in the amount of nickel on the surface with a proportionally factor α. In our simulation the etch rate R_i for monolayer i depends on the amount of nickel C_i in this monolayer. The etch time of this monolayer is equal to $1(\mathrm{ML})/R_i$. It is assumed that the nickel is removed from the surface with an efficiency γ, with $0<\gamma<1$. The total amount of nickel C_i on the surface of monolayer i is thus equal to the sum of the amount of nickel diffused in monolayer i and the fraction $(1-\gamma)C_{i-1}$, which remains on the surface after monolayer $i-1$ has been etched. The total amount of nickel diffused into the silicon is C_{tot}. This results in the following equations:

$$C_i=(1-\gamma)C_{i-1}+C_{\mathrm{tot}}\langle v(i)\rangle\times 1(\mathrm{ML}), \tag{7}$$

$$R_i=\left(\frac{\delta}{2}+\alpha C_i\right)\Phi_s(\mathrm{XeF_2}), \tag{8}$$

$$t_i=t_{i-1}+1(\mathrm{ML})/R_i. \tag{9}$$

With Eqs. (7)–(9), the etching of the contaminated layers is simulated in a computer program. To compare this model with the measurements we effectively have two independent fitting parameters: the nickel removal efficiency γ and the total amount of nickel C_{tot} diffused into the silicon. We will now compare the various experimental observations with the results of this model.

1. Nickel contamination

With this model of Eqs. (7)–(9) the data of Fig. 5 with nickel contamination as a function of the ion bombardment time T_{ion} were simulated. These measurements were done for the highest ion current and thus should best match the assumption of fast diffusion. In the simulation it is further assumed that the total amount of nickel C_{tot} is proportional to the ion bombardment time T_{ion}. The result of the simulations is shown in Fig. 10 (dotted line). The removal efficiency is set at $\gamma=0.035$ throughout. As can be seen in the figure, the model simulates the experimental data well with only two free parameters to describe all three curves.

2. Tungsten contamination

The model may also be applied to the measurements with tungsten contamination (Fig. 8 of Ref. 9). These measurements were performed with 0.5 keV $\mathrm{Ar^+}$ ions and a $\mathrm{XeF_2}$ flux of 0.6 ML/s. In the simulation the vacancy distribution for 0.5 keV $\mathrm{Ar^+}$ ions was used. During these experiments, no steady-state vacancy distribution is reached for low ion bombardment times and this has been taken into account in the simulations. In Fig. 11 the experimental data[9] and the model are presented (the y axis of Fig. 8 of Ref. 9 is rescaled to δ with other data from the article in order to compare the results of W contamination with those of Ni contamination). For these measurements the maximum enhancement saturates in time and the parameter C_{tot} is adjusted in such a way as to get the same maximum enhancement for each bombardment time. The removal efficiency is held constant at $\gamma=0.035$, which describes the decrease of the etch rate again well for long ion bombardment times.

It is seen that the position of maximum enhancement is not reproduced very well by the model. This can be explained by a limited diffusion of the tungsten causing it to be closer to the surface. One reason is that less vacancies are produced for 0.5 keV $\mathrm{Ar^+}$ ions than for 1 keV ions. Also the diffusion coefficient may be lower for tungsten. For longer bombardment times, however, the contamination has more time to move deeper into the silicon and move closer to the penetration depth of the ions. With a steady-state vacancy concentration, increasing the bombardment time does not change the vacancy concentration. Consequently, in this case when contamination moves deeper into the silicon, this is only a diffusion phenomenon with a constant diffusion coefficient. In Fig. 11 it can be seen that the positions of maxi-

mum enhancement (in XeF_2 dose) as measured and calculated with the model match better for longer bombardment times, confirming the diffusion model as the underlying mechanism of contamination transport.

Possible reaction products for W and Ni to leave the surface are WF_6 and NiF_2. As both metals show the same removal efficiency of $\gamma = 0.035$, we conclude that the volatility of WF_6 and the nonvolatility of NiF_2 do not influence the data. However, it cannot be excluded that the metals leave the surface as other reaction products.

C. Decrease in etch rate by contamination

In Figs. 4 and 6 it was shown that immediately after the ions have been switched off, the production coefficient drops below the spontaneous value δ_0 for high ion currents and high ion energy. Also the maximum enhancement decreased. This might indicate the formation of some kind of blocking layer on top of the silicon, which decreases the etch rate and the diffusion of nickel in the silicon. This process may be related to the formation of Ni_2Si, whereas the enhancement is related to atomic nickel. The product Ni_2Si is already formed at 200 °C and its heat of formation is −46.9 kJ/mol.[19] Verdonck *et al.* postulated from their experiments that the energy to form the silicide is provided by the ion bombardment.[1] Selamoglu *et al.* concluded from their measurements that fluorine might be able to extract Si from silicides and leave (in their experiment) atomic Cu on the surface.[6]

In our experiment, silicides might block the production of SiF_4, thus accounting for the low production coefficient immediately after the ions have been switched off. Once some Si has been extracted from the silicides, the production coefficient δ increases again and the Ni concentration deeper into the silicon will enhance δ even more.

These data do not provide direct evidence for the formation of silicides, but they do show that a blocking layer is possibly formed under conditions when more energy is transferred to the surface by the ions, i.e., conditions where silicides are more likely to form.

D. Difference between W and Ni contamination

From the measurements with W and Ni contamination, the enhancement due to W contamination is seen to be much larger (see Figs. 10 and 11). In order to discuss the difference between W and Ni contamination, we need to know the concentration of Ni and W.

We can estimate an upper limit for the tungsten flux from the partial pressure of WF_6. We assume a partial pressure of tungsten of 10^{-9} mbar (one tenth of the vessel pressure) as an upper limit. This results in a tungsten flux of 5.8×10^{-5} ML/s. After 25 s a maximum of 1.4×10^{-3} ML will be deposited on the surface (when the sticking coefficient is unity). This concentration results in a maximum enhancement of the production coefficient of $\delta = 0.22$.

The nickel concentration after $T_{\text{ion}} = 1000$ s was measured to be 0.01 ML at a depth of 20 ML. During this process, however, the nickel will diffuse into the silicon as described previously. We assume that no nickel was sputtered. As 20 ML is the penetration depth of the ions we conclude that 0.01 ML is a lower limit of the total amount of nickel in the silicon as more nickel may be present below the surface. Extrapolating the measured linear dependence between nickel concentration and ion bombardment time, we estimate the total concentration of nickel after 100 s ion bombardment at 1×10^{-3} ML as a lower limit. This concentration results in a maximum reaction probability of 0.18.

From these considerations we have to conclude that tungsten enhances the etch rate more than nickel. From our measurements nothing can be concluded about differences in the diffusion coefficients for tungsten and nickel.

E. Mechanism of enhancement by metal contamination

So far, only the mechanism of diffusion of the contamination has been discussed. In this section we will discuss the mechanism of the enhancement of the etch rate. Almost all impurities in silicon enhance the etch rate (see Sec. I). The most extensive study on the effect and mechanism of contamination was done in the case of F_2 etching of silicon in the presence of copper contamination.[5,6] Here, a 100-fold enhancement was measured for temperatures higher than 80 °C. Since almost no enhancement was measured in etching with atomic fluorine, a possible mechanism suggested by the authors is that Cu catalyzes the fluorination of the silicon

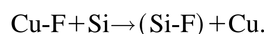

$$2\,Cu + F_2 \rightarrow 2(Cu\text{-}F),$$
$$Cu\text{-}F + Si \rightarrow (Si\text{-}F) + Cu. \qquad (10)$$

On the other hand, a mechanism involving silicide formation is favored by the same authors (Mucha *et al.* in Ref. 20), although the authors could not distinguish between these two possible catalytic cycles

$$(Cu)_s + (Si)_s \rightarrow (CuSi)_s,$$
$$(CuSi)_s + F_2 \rightarrow (Cu)_s + (SiF), \qquad (11)$$

where the subscript s indicates that the species are bound to the silicon surface. In the second reaction step of Eq. (11), Si is extracted from the silicide as shown by Selamoglu.[6] As a next step, (SiF) will react with more fluorine to form final products.

Our results, however, show an enhancement at room temperature in etching with XeF_2, which is comparable to etching with atomic F. Under these circumstances no enhancement was reported by Selamoglu *et al.*[6] This might be explained by the fact that their measurement of the etch rate by interferometry is not accurate enough to measure a small enhancement. Calculations by Chou *et al.* show that Cu forms initial stages of silicides at room temperature and weakens the bonds between surface and underlying silicon atoms on Si(111).[20] This could explain very well our results. The difference in enhancement by W and Ni can be explained by a difference in weakening of bonds.

Another difference is that our contamination diffuses into the silicon, whereas the Cu contamination of Selamoglu *et al.* was put on the surface of the silicon (by deposition, by spontaneous plating from solution or by physical rubbing of the silicon with the metal). Their measurements showed no enhancement at 185 °C for Si rubbed with Ni. This may indicate that only contamination diffused into the silicon can enhance the etch rate. This can be explained by strain around the contaminant induced by the different dimensions of the contaminants, changing the lattice parameter.[18] This stress may cause silicon bonds to break more easily and react with the fluorine. In this case, contamination catalyzes the formation of final products from fluorinated silicon. This fluorinated silicon is connected to the silicon bulk with bonds under stress. The initial fluorination takes place at dangling bonds at the surface and these bonds are not influenced by strain in the lattice. This mechanism explains both the fact that the etch rate is enhanced for a variety of contaminants and that W enhances the etch rate more than Ni because of its bigger size, thus inducing more stress in the lattice.

The mechanisms discussed in this section explain the etch rate enhancement from a totally different catalytic effect of the contamination. From our measurements we cannot distinguish between the various mechanisms, but the enhancement by silicide formation is favored.

V. REVIEW OF EARLIER WORK

In this section the effect of metal contamination on earlier publications by our group is reviewed.[8–10,21–23] As shown in the present article, the enhancement in silicon etch rate is not due to damage-enhanced etching as previously concluded,[9] but due to W contamination from the ionization gauge. The conclusions regarding this enhancement[9] should therefore be disregarded. In the other articles the ionization gauge was always switched off and the liquid nitrogen vessel was filled, thus eliminating the contamination by tungsten.

We stumbled across the nickel contamination after measurements with Ar^+ ions had been done without any signs of contamination.[8,23] It was found that the imperfect focusing of the ion beam (Fig. 7) resulted in sputtering and subsequent deposition of nickel. By adjusting the inlet pressure of Ar into the ion source, a well focused ion beam was produced and previously published results were reproduced.[24] We thus conclude that all previous articles by our group are not influenced by nickel contamination.

VI. CONCLUSIONS

We found that tungsten and nickel contamination migrates in silicon during ion-assisted etching of silicon with XeF_2 and Ar^+ ions. The mechanism of this migration is enhanced diffusion by the production of vacancies by the Ar^+ ions. As the diffusion coefficient increases with the vacancy concentration, higher ion currents move the contamination deeper into the silicon. The maximum depth for the contamination is the penetration depth of the ions. From the experiments it is concluded that nickel is migrated to a depth of 25 Å for 1 keV Ar^+ ions, in good agreement with the ion penetration depth. When etching, the contamination accumulates at the surface and enhances the spontaneous etch rate of silicon. A simple model simulates this observed behavior of enhancement for high ion currents well. Comparison of contamination with nickel and tungsten reveals that tungsten enhances the etch rate most. Traces of tungsten less than 0.01 ML may enhance the etch rate by a factor of 2. Two mechanisms for the catalytic effect of contamination are proposed, but from the experiments no distinction between the two can be made.

ACKNOWLEDGMENT

The authors would like to thank A. J. H. Maas from the Calipso setup for performing the LEIS measurements.

[1] P. Verdonck, C. M. Hasenack, and R. D. Mansano, J. Vac. Sci. Technol. B **14**, 538 (1996).
[2] T. Makino, N. Nakamura, and M. Asano, J. Electrochem. Soc. **128**, 103 (1981).
[3] L. K. White and J. Maa, Appl. Phys. Lett. **46**, 1050 (1985).
[4] P. Kongetira, G. W. Neudeck, and C. G. Takoudis, J. Vac. Sci. Technol. B **15**, 1908 (1998).
[5] N. Selamoglu, J. A. Mucha, D. L. Flamm, and D. E. Ibbotson, J. Appl. Phys. **62**, 1049 (1987).
[6] N. Selamoglu, J. A. Mucha, D. L. Flamm, and D. E. Ibbotson, J. Appl. Phys. **64**, 1494 (1988).
[7] K. Jinno, H. Kinoshita, and Y. Matsumoto, J. Electrochem. Soc. **125**, 827 (1978).
[8] M. J. M. Vugts, L. J. F. Hermans, and H. C. W. Beijerinck, J. Vac. Sci. Technol. A **14**, 2138 (1996).
[9] G. J. P. Joosten, M. J. M. Vugts, H. J. Spruijt, H. A. J. Senhorst, and H. C. W. Beijerinck, J. Vac. Sci. Technol. A **12**, 636 (1994).
[10] M. J. M. Vugts, G. J. P. Joosten, A. van Oosterum, H. A. J. Senhorst, and H. C. W. Beijerinck, J. Vac. Sci. Technol. A **12**, 2999 (1994).
[11] N. Matsunami, Y. Yamamura, Y. Itikawa, N. Itoh, Y. Kazumata, S. Miyagawa, K. Morita, R. Shimizu, and H. Tawara, At. Data Nucl. Data Tables **31**, 1 (1984).
[12] H. J. Barth, E. Mühling, and W. Eckstein, Surf. Sci. **166**, 458 (1986).
[13] S. V. Teplov, C. S. Chang, P. P. Kajarekar, T. L. Porter, and I. S. T. Tsong, Nucl. Instrum. Methods Phys. Res. B **35**, 151 (1988).
[14] H. H. Brongersma, P. A. C. Groenen and J. P. Jacobs, in *Science of Ceramic Interfaces II*, edited by J. Nowotny (Elsevier, New York, 1994), pp. 113–182.
[15] H. F. Winters, J. Vac. Sci. Technol. A **3**, 700 (1985).
[16] R. R. Hart, H. L. Dunlap, and O. J. Marsh, J. Appl. Phys. **46**, 1947 (1975).
[17] J. F. Ziegler, J. P. Biersack, and U. Littmark, *The Stopping Range of Ions in Solids* (Pergamon, Oxford, 1985), pp. 109–140.
[18] G. B. Abdullaev and T. D. Dzhafarov, *Atomic Diffusion in Semiconductor Structures* (Harwood, Chur, Switzerland, 1987), pp. 15, 38–40.
[19] S. P. Murarka, *Silicides for VLSI Application* (Academic, New York, 1983), p. 73.
[20] K. M. Lewis and D. G. Rethwisch, *Catalyzed Direct Reactions of Silicon* (Elsevier, New York, 1993), pp. 237–247, 299–331.
[21] M. J. M. Vugts, M. F. A. Eurlings, L. J. F. Hermans, and H. C. W. Beijerinck, J. Vac. Sci. Technol. A **14**, 2780 (1996).
[22] M. J. M. Vugts, G. L. J. Verschueren, M. F. A. Eurlings, L. J. F. Hermans, and H. C. W. Beijerinck, J. Vac. Sci. Technol. A **14**, 2766 (1996).
[23] M. J. M. Vugts, L. J. F. Hermans, and H. C. W. Beijerinck, J. Vac. Sci. Technol. A **14**, 2820 (1996).
[24] P. G. M. Sebel, L. J. F. Hermans, and H. C. W. Beijerinck (unpublished).